Title: Carbon flux distribution in antibiotic-producing chemostat cultures of *Streptomyces lividans*

This is the "accepted for publication" version of the article published in the journal Metabolic Engineering.

Please reference this article as: Avignone Rossa et al (2002). Carbon flux distribution in antibiotic-producing chemostat cultures of *Streptomyces lividans.* Metabol Eng **4**, 138 – 150

Authors: C. Avignone Rossa[1,#], J. White[2], A.Kuiper[1], P.W.Postma[1], M. Bibb[2], and M.J.Teixeira de Mattos[1]

Address: [1]Swammerdam Institute of Life Sciences, University of Amsterdam. Nieuwe Achtergracht 166, 1018WV Amsterdam, The Netherlands.
[2]Department of Molecular Microbiology, John Innes Centre, Colney Lane, Norwich, NR4 7UH, UK

[#]Author to whom correspondence should be addressed. **Current address**: School of Biomedical and Life Sciences, University of Surrey. Guildford, Surrey GU2 7XH, UK. Tel: (+44 1483) 686457. Fax: (+44 1483) 300374. e-mail: c.avignone-rossa@surrey.ac.uk

Abstract. The carbon metabolism of derivatives of *Streptomyces lividans* growing under phosphate-limitation in chemostat cultures and producing the antibiotics actinorhodin and undecylprodigiosin was investigated. By applying Metabolic Flux Analysis to a stoichiometric model, the relationship between antibiotic production, biomass accumulation and carbon flux through the major carbon metabolic pathways (the Embden Meyerhoff Parnas and pentose-phosphate pathways) was analysed. Distribution of carbon flux through the catabolic pathways was shown to be dependent on growth rate, as well as on the carbon and energy source (glucose or gluconate) used. Increasing growth rates promoted an increase in the flux of carbon through glycolysis and the pentose phosphate pathway. The synthesis of both actinorhodin and undecylprodigiosin was found to be inversely related to flux through the pentose phosphate pathway.

Running title: Carbon flux distribution in *Streptomyces*

Introduction

The evaluation of fluxes through metabolic pathways is an important tool for the rational improvement of microorganisms to maximize the conversion of substrates into useful end products. In Metabolic Flux Analysis, the use of a stoichiometric metabolic model incorporating all of the major intracellular reactions permits the calculation of intracellular fluxes, based on mass balances of the relevant intracellular metabolites. This approach requires knowledge of the biochemistry and physiology of the producing microorganism, and can be useful to identify specific biochemical pathways (or parts thereof) that can be targeted for genetic manipulation (Bailey 1991; Stephanopoulos and Vallino 1991). Detailed discussions of the theory of Metabolic Flux Analysis can be found in Vallino and Stephanopoulos (1990), Savinell and Palsson (1992), van Gulik and Heijnen (1995), and Stephanopoulos *et al*. (1998).

Although Metabolic Flux Analysis has been applied to an extensive number of genera, thus far there have been only two reports applying Metabolic Flux Analysis to *Streptomyces* species. Daae and Ison (1999) presented a theoretical sensitivity assessment of a biochemical network for *S. lividans*, analysing how the estimation of intracellular fluxes is affected by perturbations in the measured fluxes and in the composition of the biomass. Their analysis showed that changes of up to 20% in the level of biomass precursors do not affect the estimation of intracellular fluxes significantly, and that oxygen consumption has the greatest impact on flux calculation. Employing experimental data from the literature, Naeimpoor and Mavituna (2000) applied metabolic flux analysis to cultures of *S. coelicolor* under different nutrient

limitations. The biochemical network developed was underdetermined, and therefore the system could only be solved by applying several constraints. Using this approach, nitrogen limitation appeared to give the highest specific actinorhodin production rate and the lowest maintenance energy, although it was accompanied by the highest specific production rate of other primary metabolites.

Carbon flux distribution in antibiotic producing *Streptomyces* species has also been studied by using radiorespirometry and radio-labelling techniques. Dekleva and Strohl (1988a, 1988b) showed that carbon from glucose is incorporated into the polyketide ε-rhodomycinone via the EMP pathway, with a minor contribution of the pentose-phosphate pathway, and identified acetyl-CoA as the precursor of the antibiotic by *Streptomyces* C5. Obanye *et al*. (1996) studied the correlation between the production of the cyclopentanone antibiotic methylenomycin and the flux of carbon through the pentose phosphate pathway in batch cultures of *Streptomyces coelicolor* A3(2), reporting an increase in flux through the pentose phosphate pathway when synthesis of the antibiotic started.

We have applied the technique of Metabolic Flux Analysis to the carbon metabolism of *Streptomyces lividans* producing two different antibiotics: the polyketide actinorhodin (ACT) and the tripyrrole undecylprodigiosin (RED). The biosynthetic pathways of these two compounds share many characteristics with those of other secondary metabolites. ACT is derived from the intermediate acetyl-CoA, which serves as a precursor in the synthesis of numerous antibiotics (Herbert 1989). In contrast, the tripyrrole

nucleus of RED is derived from pyruvate and the amino-acids proline, serine and glycine. Many important secondary metabolites contain amino acid residues in their molecules, including the calcium-dependent peptide antibiotic (CDA) of *S. coelicolor* , the vancomycin group of antibiotics, and the actinomycins, among many others (Hodgson 2000). Thus we believe that the understanding derived from rationally analysing -and improving- ACT and RED production by *S. lividans* will be applicable to many other streptomycetes and their products. In this study, phosphate-limited chemostat cultures of *S. lividans*, grown at various dilution rates and with either glucose or gluconate as carbon source, were used to obtain steady state values of accumulation rates, which were employed to estimate the carbon flux distribution under different physiological conditions.

Our results show that changing growth conditions (growth rates and carbon source) promote variations in the distribution of carbon fluxes among the main metabolic pathways, and that the production of ACT and RED can be linked to a decrease in the flux through the pentose phosphate pathway. Given that the primary metabolism of different *Streptomyces* species is highly conserved, the stoichiometric model we have derived for *S. lividans* should be generally applicable for Metabolic Flux Analysis of antibiotic production in other streptomycetes, provided, of course, that appropriate modifications, such as the steps involved in the biosynthesis of the particular antibiotic under study and the specific co-factor requirements, are introduced.

Materials and methods

Strains. *S. lividans* RpdS102, RpdS103, and RpdS105 were employed throughout this work. All strains are derivatives of *S. lividans* 1326. RdpS102 contains the pathway-specific regulatory gene *act*II-ORF4 cloned on the pIJ101-derived multicopy plasmid pIJ68 (Passantino *et al*. 1991), and overproduces ACT. RpdS103 contains the pathway-specific regulatory gene *redD* cloned on the pIJ101-derived multicopy plasmid pIJ6014 (Takano *et al*. 1992), and overproduces RED. RpdS105 contains the pIJ101-derived plasmid vector pIJ486 (Ward *et al*. 1986), and was used as a vector only control.

Stock cultures. Aliquots (1 ml) of spore suspensions of the strains were kept at -70 °C (the master cell bank). Mycelial suspensions were prepared from these, and 1 ml aliquots, kept at -70 °C (the working cell bank), were used as starting inocula.

Growth conditions and media. Inocula were prepared following a two step procedure. Mycelia from the working cell bank were used to inoculate 100 ml GG1 medium in a 500 ml Erlenmeyer flask. The medium was agitated to promote dispersed growth by using a magnetic stirrer and a triangular magnetic bar. After incubation at 28 °C for 48 h, 8 ml of the culture were transferred to a 500 ml Erlenmeyer flask containing 100 ml GYB medium, and incubated at 28 °C for 24 h.

Medium GG1 contained ($g.l^{-1}$): glucose, 15; glycerol, 15; soya peptone, 15; NaCl, 3; $CaCO_3$, 1. Medium GYB contained ($g.l^{-1}$): glucose, 33; yeast extract,

15. The pH of each medium was adjusted to 7.0 by addition of 4N NaOH before sterilisation.

Chemostats: Cells were grown in phosphate-limited chemostats in a modified Evans medium, with nitrate as the nitrogen source. The medium contained (mM): NaH_2PO_4, 10; KCl, 10; $MgCl_2$, 1.25; $NaNO_3$, 100; Na_2SO_4, 2; citric acid, 2; $CaCl_2$, 0.25; carbon source, 140. 5 ml of the following trace element stock solution was added to each litre of medium (mM): ZnO, 50; $FeCl_3$, 20; $MnCl_2$, 10; $CuCl_2$, 10; $CoCl_2$, 20; H_3BO_3, 10; Na_2MoO_4, 0.02; HCl, 100. Foam formation was prevented by the automatic addition of 10% (v/v) antifoam agent suspension (BDH Laboratory Supplies, UK), at a fixed rate of 0.45 ml h^{-1}.

Starvation experiments: Addition of fresh medium to steady state phosphate-limited chemostats was stopped, and carbon source immediately added to a final concentration of 140 mM. Samples were taken every 12 h, until the carbon source could not be detected in the culture supernatant.

Bioreactors (750 ml working volume, Applikon) were inoculated with 50 ml of the GYB grown culture. pH was controlled at 6.8 $\pm$ 0.2 by the automatic addition of either 2 N NaOH or 2 N HCl. Temperature was controlled at 28 °C. The agitation rate was set at 1000 rpm, and the air flow rate at 1.25 $l \cdot min^{-1}$. Cells grew in a dispersed fashion (as assessed by microscopic observation) throughout the fermentation period (approximately 500 h). Steady states were assumed to be reached after 7 volume changes in the bioreactor.

Analytical procedures: Steady state samples taken from the bioreactor were centrifuged for 10 min at 5000 rpm at 4 °C, and the supernatants frozen at -20 °C for subsequent analysis.

Dry weight determinations: 10 ml aliquots of culture were centrifuged (5000 g, 10 min), the pellets washed and centrifuged twice with deionized water, and then placed at 105 °C for approximately 24 h, until the weight remained constant.

HPLC: Supernatants were deproteinized by acid precipitation with 35% $HClO_4$ (0.1 ml to 1 ml supernatant) and neutralized with cold 7 N KOH. After centrifugation (4 min at 10000 rpm), the supernatants were filtered through a 0.22 μm membrane. Residual carbon source, pyruvate and lactate concentrations were determined by HPLC using an LKB 2142 refractive index detector. The filtered supernatants were injected into an Aminex HPX 87H organic acid analysis column (BioRad), at 65° C. The eluent was 5 mM H_2SO_4 at a flow rate of 0.5ml·h^{-1}.

Enzymatic determinations: Standard enzymatic methods were used for the determination of α-oxoglutarate (Bergmeyer and Bent 1974), citrate (Dagley 1974), nitrate, and ammonium (Boehringer Mannheim, Methods of Biochemical Analysis and Food Analysis, 1989) in non-deproteinized supernatants.

Enzyme assays: Phosphoenolpyruvate carboxylase activity was measured in cell free extracts as described by Dekleva and Strohl (1988a). The presence of the enzyme nicotinamide nucleotide transhydrogenase was assayed as described by Vallino and Stephanopoulos (1994).

Gas composition: The composition of the exhaust gas with respect to O_2 and CO_2 was determined using a paramagnetic gas analyser (Servomex analyser) and an infrared gas analyser (Servomex IR analyser PA404).

Actinorhodin: ACT was determined on whole broths. Two ml of whole broth were treated with 1 ml 3N KOH, vortexed until the biomass appeared totally disrupted, and centrifuged (15 min, 5000 rpm). The absorption of the blue supernatant was determined at 640 nm. The concentration of ACT was calculated on the basis of a molar absorption coefficient of 25320 $M^{-1} \cdot cm^{-1}$ (Bystrykh *et al*. 1996).

Undecylprodigiosin: RED was determined by resuspending the mycelial pellet in CH_3OH-HCl (pH = 1.5) and vortexing until total disruption of the biomass. The suspension was centrifuged (15 min, 5000 rpm), and the absorbance of the supernatant was measured at 530 nm. The concentration of RED was calculated on the basis of a molar absorption coefficient of 100500 $M^{-1} \cdot cm^{-1}$ (Tsao *et al*. 1985).

Production rates of biomass, CO_2, NH_4^+, citrate, pyruvate, lactate, α-oxoglutarate, and ACT/RED, as well as consumption rates of carbon source, O_2, and NO_3^-, were calculated. In the starvation experiments, rates were calculated as the difference between the concentrations of the measured metabolite at time t and at time $t+\Delta t$, divided by the length of the period considered, Δt, and corrected for changes in biomass concentration.

Metabolic Flux Analysis. The biochemical stoichiometric network developed for this system consists of 36 or 38 pathway reactions, involving 46 or 47

compounds, depending on the carbon source employed (See Appendix). The difference between our model and the one presented by Daae and Ison (1999) is that we have included the steps for ACT and RED biosynthesis. We have combined several steps in some of the amino-acid biosynthesis pathways, leaving out a number of intermediates to obtain a model with fewer reactions.

Reactions of primary metabolism. The stoichiometric equations for glycolysis, the tricarboxylic acid cycle (TCA), and the pentose phosphate pathway (PPP) were collected from literature related to different species of *Streptomyces* (Salas *et al.* 1984; Surowitz and Pfister 1985; Dekleva and Strohl 1988a, 1998b). These appear to be the most important pathways for glucose metabolism in *S. coelicolor* (Alves 1997; Hodgson 2000), a species closely related to *S. lividans*. The Entner-Doudoroff pathway is non functional in several species of *Streptomyces*, including *S. lividans* (Dekleva and Strohl 1988b). Poor growth in C-2 substrates and lack of activity of isocitrate lyase and malate synthase are indicative of the absence of the glyoxylate shunt in *Streptomyces lividans* (Dekleva and Strohl 1988b; Hodgson 2000). Therefore, neither the Entner-Doudoroff pathway nor the glyoxylate shunt were considered in this model. The presence of an ATP-dependent glucokinase in *S. lividans* has been demonstrated by Ikeda *et al*. (1984) and Titgemeyer *et al*. (1995), whereas only a fructose-specific PEP:PTS system could be found (Titgemeyer *et al*. 1995), which is apparently not essential for uptake and phosphorylation of fructose (Butler *et al*. 1999). Consequently, we have assumed that the phosphorylation of glucose is carried out by an ATP-dependent glucose kinase. The carboxylation of phosphoenol-pyruvate was

confirmed by measurements of phosphoenolpyruvate carboxylase activity in cell extracts obtained from the cultures. This is the only enzyme involved in anaplerotic reactions in streptomycetes (Hodgson 2000). Although a gene putatively encoding the enzyme nicotinamide nucleotide transhydrogenase, reversibly reducing NADP at the cost of NADH, has been identified in the genome sequence of *S. coelicolor*, experiments in cell-free extracts failed to show this activity in the strains of *S. lividans* used in this work, and therefore was not included in the model. This leaves the pentose phosphate pathway and the TCA cycle enzyme isocitrate dehydrogenase, which converts isocitrate to α-oxoglutarate, as the major sources of NADPH, which serves as the reducing agent for the synthesis of antibiotic precursors.

Amino acid biosynthesis. The amino acid biosynthetic pathways considered were only those involved in biomass production and/or in the synthesis of the product(s) of interest. Amino acid biosynthetic pathways in streptomycetes appear to be the same as those present in other bacteria (Hodgson 2000) and therefore their stoichiometries were assumed to be the same as those reported for other microorganisms (Gottschalk 1986).

ACT and RED biosynthesis. The reactions leading to the synthesis of ACT and RED were grouped together into single reactions; that is, no intermediates were considered. The polyketide ACT is derived from acetyl-CoA (Gorst-Allman *et al*. 1981; Katz and Donadio 1993), whereas the tripyrrole RED is derived from pyruvate, proline, serine, and glycine (Wasserman *et al*. 1974). The demand for NADPH assumed in ACT biosynthesis was based on the known features of polyketide biosynthesis. Polyketides are synthesised in a series of reactions that resemble fatty acid

synthesis, differing in the post-termination processes (reductions, hydroxylations, etc.) occurring to the acyl chain (Katz and Donadio 1993). Strohl *et al*. (1989) studied various species of *Streptomyces* and demonstrated that cell extracts require NADPH for the complete synthesis of anthracylines, compounds structurally related to actinorhodin, and that NADH cannot replace NADPH in at least two reactions of the sequence. The biosynthetic pathways of anthracycline and actinorhodin have been proposed to be similar (Strohl and Connors 1992). Recently, Rajgarhia *et al*. (2001) showed that the cell-free extracts of *S. lividans* containing the genes for daunorubicin synthesis failed to synthesise this polyketide when NADPH was left out of the reaction mixture. Furthermore, the presence of NADPH-dependent oxidoreductases involved in antibiotic biosynthesis has been reported in other *Streptomyces* species (Parry and Li 1997).

Biomass synthesis. In the absence of information regarding precursor requirements for biomass accumulation in *Streptomyces*, the stoichiometric equation for biomass synthesis in *E. coli* (Ingraham *et al*. 1983) was used. This approach has been employed successfully for flux analysis in several microorganisms (Vallino and Stephanopoulos 1990; Goel *et al*. 1993), including the actinomycete *Streptoverticillium mobaraense* (Zhu *et al*. 1996; Zhu *et al*. 1998). Moreover, the sensitivity analysis of Daae and Ison (1999) showed that variations as high as 20% in the biomass composition of *S. lividans* do not affect flux estimation.

Further details of the bioreaction network are presented in the Appendix.

Results

Chemostat and starvation experiments. To quantify the effect of growth rate on product formation, all strains were grown in chemostat cultures at various dilution rates, including zero dilution (starvation experiments), to obtain conditions approaching fed batch cultures in which the growth rate is extremely low. Several studies suggest an important role for the pentose phosphate pathway in antibiotic production in *Streptomyces* species (Dekleva and Strohl 1988b; Obanye *et al*. 1996). This was assumed to reflect a requirement for NADPH for the synthesis of the precursors needed for secondary metabolism. Therefore, both glucose and gluconate were studied as carbon and energy sources, with the expectation that the relative activity of the NADPH generating pentose-phosphate pathway would increase with gluconate as the carbon and energy source. All cultures were phosphate-limited since ACT production in *S. coelicolor* A3(2) is known to occur upon phosphate depletion (Doull and Vining 1990). Since ammonium represses RED production (J.W. and M.J.B, unpublished results; Ives and Luiten, pers. comm.), nitrate was used as nitrogen source. The inputs to the stoichiometric model were the rates of biomass, CO_2, ACT, RED, and organic acid (pyruvate, citrate, α-oxoglutarate, and lactate) production, and carbon source, nitrogen source and O_2 consumption.

Tables 1 and 2 present the results obtained in chemostats at three different dilution rates (namely, 0.05 h^{-1}, 0.1 h^{-1}, and 0.15 h^{-1}), while the results of starvation experiments are presented in Tables 3a and 3b. All experiments were performed three times, and steady states were sampled in triplicate. The

results presented are the mean values from these experiments. Carbon balances of 100 $\pm$ 5% were obtained in all of the experiments reported.

In glucose fed chemostats (Table 1), upshifts in dilution rate promoted a significant decrease in the steady state biomass concentration of the ACT overproducing strain 102 and the RED overproducing strain 103, but this was less so for the reference strain 105. For all strains, excretion of organic acids was found to be very low (< 10^{-3} milli C-mole $\times$ (g biomass $\times$ h)$^{-1}$) or below the detection limit. Specific ACT production remained constant in strain 102 upon a change in dilution rate from 0.05 h^{-1} to 0.1 h^{-1}, but dropped for the highest dilution rate tested. For strain 103, the highest specific production rate of RED was found at D = 0.1 h^{-1}. Control strain 105 produced no detectable ACT, and approximately ten-fold lower levels of RED compared to the RED-overproducing strain 103.

With gluconate-grown cells (Table 2), an increase in dilution rate promoted a decrease in biomass concentration, as it did for the glucose grown cells. But in many other aspects, the cultures performed quite differently. Firstly, biomass yields (*i.e.*, the amount of biomass per amount of substrate consumed) were lower than those observed with glucose. Secondly, the excretion rates of organic acids were significant in most cases. And thirdly, with gluconate, ACT yields from strain 102 were 7 to 10 times lower than those obtained with glucose, whereas RED yields (strain 103) were higher.

In general, fed-batch conditions are used for industrial production systems. One important feature of such a method is that a low production rate of biomass can be achieved. To mimic this, starvation experiments were

performed. Under these conditions, a significant proportion of the carbon source was directed towards the production of organic acids, mostly pyruvic and citric acid, and a higher product (ACT, RED) formation rate was detected compared to the chemostat cultures. The production rates in these experiments were extremely low: the maximum concentration of product was reached at 48 h. Apart from the differences in product concentration, the extracellular metabolite profile was not affected, implying that the stoichiometric model used for the chemostat experiments could be used also for the non-growth experiments. A similar situation was found by Jørgensen *et al*. (1995) in the analysis of metabolic fluxes in fed-batch cultures of *Penicillium chrysogenum*.

The calculated fluxes and yield values are presented in Tables 3a and 3b.

Product yields. The percentage of carbon converted into product appeared to be different under the different growth conditions and carbons sources tested. The experimental yield values ($Y_{P/S}$) are presented in Tables 1-3. At zero growth rate with glucose as carbon and energy source, 14% of the glucose consumed was converted into ACT. This yield decreased to 0.6% at the highest dilution rate, whereas yields of RED ranged from 2.4% to 0.01%. With gluconate, yield values followed the same trend. However, the values were much lower than those observed with glucose. Carbon conversions to ACT ranged from 1.6% to 0.02%, whereas for RED they ranged from 3.3% to 0.01%. Interestingly, in contrast to the results obtained with glucose, $Y_{P/S}$ with gluconate was higher for RED than for ACT.

Metabolic flux analysis. A simplified version of the metabolic network is presented in Fig 1 showing only those fluxes involved in generating energy and/or reducing power, and ACT and RED. The results obtained were analysed using the stoichiometric model outlined above. Intracellular fluxes for all reactions present in the metabolic network were calculated. The values obtained for those fluxes are expressed in milli C-mole $\times$ (g biomass $\times$ h)$^{-1}$. To be able to compare the results obtained with the different carbon sources, we defined the following fluxes: $X_{GLUCOSE}$ or $X_{GLUCONATE}$: flux of the carbon sources through the uptake system(s) (reactions 1 or 1a, see Appendix); $X_{GLYCOLYSIS}$: flux through the step converting glyceraldehyde 3-phosphate to 3-phosphoglycerate (reaction 4); X_{PPP}: sum of the fluxes through the reactions converting ribulose 5-phosphate to ribose 5-phosphate (reaction 18) and to xylulose 5-phosphate (reaction 19); X_{TCA}: flux through the reaction condensing acetyl-CoA and oxaloacetate to citrate (reaction 9); X_{ACT} or X_{RED}: flux towards the products ACT (reaction 36a) or RED (reaction 36b).

Figures 2A and 2B show the distribution of the fluxes $X_{glucose}$, X_{PPP}, and X_{ACT} or X_{RED} observed for strains 102 and 103, respectively, over the range of growth rates studied, with glucose as the carbon source. The values of X_{RED} in the control strain 105 are also presented to show the lower percentage of carbon directed to secondary metabolism in a strain which is not over-producing antibiotics. Under the non-growth conditions obtained in the starvation experiments, virtually no PPP activity is observed. This means that $X_{GLYCOLYSIS}$ is almost equal to $X_{GLUCOSE}$, or, in other words, all carbon is catabolized through glycolysis. The increase of X_{PPP} with the increase in

growth rate may reflect the need for a higher turnover of NADPH and precursors derived from the PPP, such as ribose 5-phosphate and erythrose 4-phosphate, for biomass synthesis (See reaction 34 in the Appendix). X_{ACT} and X_{RED} decrease 6- and 15- fold, respectively, with increasing growth rates in the range from starvation ($D \approx 0$) to $D = 0.15\ h^{-1}$, and are about two orders of magnitude higher than in the control strain 105. Higher growth rates (that is, increasing carbon flux towards biomass synthesis) promote an increase in carbon uptake ($X_{GLUCOSE}$) and $X_{GLYCOLYSIS}$ (Table 4). The calculated ratios of TCA flux and glycolytic rate ($X_{TCA}/X_{GLYCOLYSIS}$) are a consequence of carbon being drained off the Embden Meyerhof Parnas pathway (EMP) towards biomass synthesis and acid excretion. In the steady state experiments with strain 102, $X_{TCA}/X_{GLYCOLYSIS}$ values were within the range 0.6 – 0.7 (Table 4), whereas for strain 103 these values ranged from 0.7 to 0.8. A decrease of X_{ACT} and X_{RED} with X_{PPP} was observed (Figure 3). The high demand for precursors for biomass synthesis may reduce their availability for antibiotic biosynthesis, resulting in the observed decrease in X_{ACT} and X_{RED}.

The stoichiometry deduced for ACT synthesis (Reaction 36a) shows a relatively high demand for NADPH, which may affect the flux distribution especially in the experiments with the highest yields of the antibiotic. This was tested by calculating flux distributions with the experimental results presenting the highest yields of ACT, using NADPH consumption values ranging from 0 to 1 mole NADPH per C-mole ACT. Compared to the X_{PPP} value estimated using the stoichiometry shown in Reaction 36a (*i.e.* 0.875 mole NADPH per C-mole ACT), X_{PPP} decreased 7% for a NADPH demand of 0, whereas for a

maximum demand of 1 mole per C-mole NADPH, X_{PPP} increased only 1%. This means that the relatively high NADPH requirements for ACT are not likely to affect the calculation of fluxes.

In the control strain 105 grown on glucose, $X_{GLUCOSE}$ and X_{PPP} followed a similar trend to those observed in strains 102 and 103, although the values for X_{PPP} were slightly lower, as mentioned previously. This implies that the expression of genes involved in ACT and RED biosynthesis does not promote any noticeable change in the regulation of the major carbon metabolic pathways. However, in the starvation experiment $X_{GLUCOSE}$ was much higher than at the lowest steady state growth rate.

All three strains were also grown with gluconate as carbon source in an attempt to impose carbon fluxes that were different to those occurring with glucose. Gluconate is phosphorylated to 6-phosphogluconate, which is able either to enter the pentose phosphate pathway yielding ribulose 5-phosphate (reaction 1b), or to be converted into glucose 6-phosphate (reaction 1c), which is then metabolised through glycolysis. The Metabolic Flux Analysis performed on these cultures showed, for every condition tested, that the flux through the step which converts 6-phosphogluconate to glucose 6-phosphate (reaction 1c) is zero, and that the reaction catalysed by the glucose 6-phosphate isomerase (reaction 2) proceeds in the direction of glucose 6-phosphate, which then enters the pentose phosphate pathway.
With gluconate as carbon source (Fig 2C and 2D), fluxes through the PPP are higher than those calculated from the experiments with glucose, and increase

with increasing growth rate. Some of the fluxes through the PPP are higher than the input flux ($X_{GLUCONATE}$). This can be explained because part of the carbon which goes through the PPP towards glycolysis (Fructose 6P) is directed to glucose 6-phosphate, which re-enters the PPP. Our definition of X_{PPP} does not consider this recycling of carbon. The ratio $X_{TCA}/X_{GLYCOLYSIS}$ (Table 4) is generally lower for growth on gluconate than it is for growth on glucose, reflecting the elevated acid production rates with the former substrate. It ranges from 0.43 to 0.48 in strain 102, showing a minimum at D = 0.1 h^{-1} (which coincides with the peak in acid excretion for this strain growing on gluconate). In strain 103, this ratio varies from 0.35 to 0.45 in the steady state experiments, but is as low as 0.2 in the starvation experiment (Table 4). As with growth on glucose, X_{ACT} and X_{RED} achieve the highest values at the lowest X_{PPP} calculated (Fig 3B), although the trend line for the two conditions is different.

Strain 105 shows a different behaviour. As observed for the other strains and conditions, the increase in growth rate promotes an increase in X_{PPP} and $X_{GLYCOLYSIS,}$ but a decrease in X_{TCA}, which results in the $X_{TCA}/X_{GLYCOLYSIS}$ ratios ranging from 0.65 to 0.04 (Table 4).

Discussion

The objective of our study was to quantify the distribution of intracellular carbon fluxes in *S. lividans* grown under well-defined conditions and to relate them to optimal conditions for the production of secondary metabolites, hence potentially identifying bottlenecks that may hamper the latter's biosynthesis.

This was achieved by applying Metabolic Flux Analysis to various chemostat cultures and starvation experiments of strains which had an increased capacity to produce either RED or ACT.

The distribution of fluxes over glycolysis, the pentose phosphate pathway and to ACT and RED production was affected by both the growth rate and the nature of the carbon and energy source. For the same growth rate, higher fluxes through the pentose phosphate pathway were found invariably with gluconate cultures than with glucose cultures. From the Metabolic Flux Analysis we conclude that for both glucose and gluconate grown cells, an increase in growth rate is accompanied by increased flux through the pentose phosphate pathway. Under conditions in which the growth rate approximated zero, the pentose phosphate pathway flux was found to be virtually zero. These latter experiments do not represent a true steady state, but according to Stephanopoulos *et al.* (1998), transient experiments can be used to obtain intracellular flux distributions. In our case, these cultures approximate to chemostat experiments with D = 0, and they were carried out to extend the flux analysis to conditions that approach actual production conditions (*i.e.* low biomass accumulation).

The increase in X_{PPP} with increased growth rate was also reported for *Aspergillus nidulans* (Stephanopoulos *et al*. 1998), and has been explained by an increased demand for NADPH and precursor metabolites for biomass synthesis. The same authors reported that the increase in X_{PPP} was accompanied by a decrease in glycolytic flux, as determined by the decrease in aldolase activity *in vitro*. In our experiments, the $X_{GLYCOLYSIS}/X_{PPP}$ ratio decreased with increasing growth rates, when gluconate was the carbon

source. In contrast, this ratio was constant over the range of steady states when glucose was used as carbon source, implying a proportional increase of $X_{GLYCOLYSIS}$ and X_{PPP} with increased growth rate. Our definition of $X_{GLYCOLYSIS}$ as the flux through the step converting glyceraldehyde 3-phosphate into 3-phosphoglycerate allowed us to compare the results obtained with the two different carbon sources. However, had we defined $X_{GLYCOLYSIS}$ as the step converting glucose 6-phosphate into fructose 6-phosphate (reaction 2, see Appendix), a decrease of $X_{GLYCOLYSIS}/X_{PPP}$ with increasing growth rates would have been observed in the glucose fed chemostats, in agreement with the results presented by Stephanopoulos *et al*. (1998).

A strong negative effect of increasing growth rate on the flux of carbon to secondary metabolites was observed with both carbon sources. The PPP activity increases when the demand for NADPH and precursors for biomass synthesis is enhanced (that is, at higher growth rates). The values observed for X_{PPP} ranged from 25 to 40% of the carbon input, except for the cultures at very low growth rates. This is in accordance with values reported for other streptomycetes using radio-labelling or radiorespirometry: Dekleva and Strohl (1988b) reported an X_{PPP} of appr. 30%, using radio-labelling techniques, and Obanye *et al*. (1996) found a wide range of X_{PPP} to $X_{GLYCOLYSIS}$ ratios. From those data, it can be estimated that X_{PPP} ranged from 18% to 52%. The biosynthesis of ACT requires NADPH, which is also required for the synthesis of RED precursors. Expressed in C-mole, the requirements for 3-phosphoglycerate, glutamate, and pyruvate to synthesise one gram of RED, and for acetyl-CoA to synthesise one gram of ACT, are more than 10 times higher than the requirements for the same precursors to synthesise one gram

of biomass. However, the values for X_{PPP} observed for the ACT and RED overproducing strains were only slightly (5%) higher than those of the control strain, which can be considered to reflect basal PPP fluxes. The increased X_{PPP} observed at the lower growth rates in the ACT and RED overproducing strains can be attributed to the demand for carbon and NADPH for RED or ACT synthesis, whereas the decrease at lower dilution rates implies that these demands can be met by the basal metabolic activity of the organism. This may suggest that ACT or RED are synthesised only when a surplus of precursors is present. Hutchinson *et al*. (1993) have proposed that precursor availability may be a limiting factor in the synthesis of polyketides.

The negative correlation between biomass formation (growth) and ACT or RED synthesis found by us is in good agreement with the results of Dekleva and Strohl (1988b). These workers showed that carbon incorporated into ε-rhodomycinone in *Streptomyces* C5 derives mainly from the glycolytic pathway, with a minor contribution of the PPP. The biosynthetic pathway for this secondary metabolite is supposedly similar to that of ACT, involving malonyl-CoA as an intermediate. Methylenomycin production by *S. coelicolor* is accompanied by a two fold increase of flux through the PPP (Obanye *et al*. 1996) and its NADPH-dependent synthesis is accompanied by a decrease in the $X_{TCA}/X_{GLYCOLYSIS}$ ratio. This is consistent with a drain of acetyl-CoA (an intermediate in methylenomycin synthesis) from the Embden Meyerhof Parnas Pathway. Similar observations were made with respect to the synthesis of spiramycin by *S. ambofaciens*, where pyruvate is drained from the Embden Meyerhof Parnas Pathway to yield, in that case, malonyl-CoA (Laakel *et al*. 1994). The flux analysis of *S. coelicolor* presented by Naeimpoor

and Mavituna (2000) cannot be readily compared to the results presented here. In this earlier paper, there is no description of the metabolic network, and several stoichiometric and experimental constraints are used to solve the underdetermined system obtained.

In conclusion, the relationship between carbon flux through the main metabolic pathways and the production of biomass, RED and ACT was analysed. An increased production rate of biomass will require a larger fraction of carbon to be directed towards growth precursors and demands an enhanced turnover of the major biosynthetic redox carrier NADPH. Thus under conditions of nutrient availability, biomass synthesis and secondary metabolite production compete for common substrates, with the former favoured, reflecting regulatory mechanisms at the level of gene expression, or differences in the kinetics of the relevant enzymes. This finding can be exploited for antibiotic production by using a culture system (such as fed-batch) in which a low biomass synthesis rate is maintained.

No significant differences between the catabolic fluxes in the control strain and in the overproducing strains were observed (*i.e.* no differences in biomass yields were found). This suggests that ACT or RED production does not constitute an energetic burden compared to biomass production. From the results discussed here, we can predict that strains with an impaired pentose phosphate pathway would result in lower biomass yields but probably higher ACT/RED yields.

We show here that ACT and RED production correlate negatively with PPP activity. However, we manipulated the PPP activity by imposing changes in biomass production. Experiments with inducible strains, in which ACT/RED production is triggered under steady state conditions, are currently being performed. Such experiments will allow us to assess how central metabolic fluxes are affected upon an increase in the synthesis of these two secondary metabolites.

Acknowledgements. This work was supported by EU grant BIO4960332. The authors would like to thank Prof D. Levine (Norwegian University of Science and Technology, Trondheim, Norway) for his valuable comments.

References

- Alves, A.M. (1997). Regulation of glucose metabolism in the actinomycetes *Amycolatopsis methanolica* and *Streptomyces coelicolor* A3(2). Doctoral Thesis, University of Groningen, The Netherlands.
- Bailey, J.E. (1991) Towards a science of metabolic engineering. Science **252**, 1668-1674.
- Bergmeyer, H. U., and Bent, E. (1974). 2-oxoglutarate UV spectrophotometric determination. *In* "Methods of enzymatic analysis" (Bergmeyer, H. U., Ed), 3rd Ed, pp. 1577 – 1580, Verlag Chemie, Weinheim.
- Butler, M.J., Deutscher, J.; Postma, P.W., Wilson, T.J.G., Galinier, A., and Bibb, M.J. (1999). Analysis of a *pts*H homologue from *Streptomyces coelicolor* A3(2). FEMS Microbiol. Lett. **177**, 279 – 288.
- Bystrykh, L.V., Fernández-Moreno, M.A., Herrema, J.K., Malpartida, F., Hopwood, D.A., and Dijkhuizen, L. (1996). Production of actinorhodin related "blue pigments" by *Streptomyces coelicolor* A3(2). J. Bacteriol. **178**, 2238-2344.
- Daae, E.B., and Ison, A.P (1999). Classification and sensitivity analysis of a proposed primary metabolic reaction network for *Streptomyces lividans*. Metabolic Engineering **1**, 153 – 165.
- Dagley, S. (1974) Citrate. UV spectrophotometric determination. *In* "Methods of enzymatic analysis" (Bergmeyer, H. U., Ed.), 3rd Ed, pp. 1562 – 1565, Verlag Chemie, Weinheim.

- Dekleva, M.L., and Strohl, W.R. (1988a). Activity of phosphoenolpyruvate carboxylase of an anthracycline-producing streptomycete. Can. J. Microbiol. **34**: 1241-1246.
- Dekleva, M.L., and Strohl, W.R. (1988b). Biosynthesis of ε-rhodomycinone from glucose by *Streptomyces* C5 and comparison with intermediary metabolism of other polyketide-producing streptomycetes. Can. J. Microbiol. **34**: 1235-1240.
- Doull, J.L., and Vining, L.C. (1990). Nutritional control of actinorhodin production by *Streptomyces coelicolor* A3(2): suppressive effects of nitrogen and phosphate. Appl Microbiol Biotechnol **32**: 449 - 454
- Goel, A., Ferrance, J., Jeong, J., and Ataai, M.M. (1993). Analysis of metabolic fluxes in batch and continuous cultures of *Bacillus subtilis*. Biotech. Bioeng. **42**, 686-696.
- Gorst-Allman, C.P., Rudd, B.A.M., Chang, C-j., and Floss, H.G. (1981). Biosynthesis of Actinorhodin. Determination of the point of dimerization. J. Org. Chem. **46**, 456-458.
- Gottschalk, G. (1986). Bacterial metabolism. Springer Verlag, New York, USA.
- Herbert, R. B. (1989). The biosynthesis of secondary metabolites, 2nd ed., Chapman and Hall, London.
- Hodgson, D.A. (2000). Primary metabolism and its control in Streptomycetes: A most unusual group of bacteria. Adv. Microb. Phys. **42**, 47 – 238.

- Hutchinson, C.R., Decker, H., Madduri, K., Otten, S.L., and Tang, L. (1993). Genetic control of polyketide biosynthesis in the genus *Streptomyces*. Antonie van Leeuenhoek **64**, 165 – 176.
- Ikeda, H., Seno, E.T., Bruton, C.H., and Chater, K.F. (1984). Genetic mapping, cloning and physiological aspects of the glucose kinase gene of *Streptomyces coelicolor*. Mol. Gen. Genetics **96**, 501 – 507.
- Ingraham, J.L., Maaløe, O., and Neidhardt, F.C. (1983). Growth of the bacterial cell. Sinauer Associates, Sunderland, MA, USA.
- Jørgensen, H., Nielsen, J., Villadsen, J., and Møllgard, H. (1995). Metabolic flux distribution in *Penicillium chrysogenum* during fed-batch cultivations. Biotech. Bioeng. **46**, 117-131.
- Katz, L., and Donadio, S. (1993) Polyketide synthesis: Prospects for hybrid antibiotics. Annu. Rev. Microbiol. **47**, 875-912.
- Laakel, M., Lebrihi, A., Khaoua, S., Schneider, F., Lefebvre, G., and Germain, P. (1994). A link between primary and secondary metabolism: malonyl-CoA formation in *Streptomyces ambofaciens* growing on ammonium ions or valine. Microbiology **140**, 1451 – 1456.
- Naeimpoor, F., and Mavituna, F. (2000). Metabolic Flux Analysis in Streptomyces coelicolor under various nutrient limitations. Metabolic Engineering **2**, 140 – 148.
- Obanye, A.I.C., Hobbs, G., Gardner, D.C.J., and Oliver, S.G. (1996). Correlation between carbon flux through the pentose phosphate pathway and production of the antibiotic methylenomycin in *Streptomyces coelicolor* A3(2). Microbiology, **142**, 133-137.

- Parry, R.J., and Li, W. (1997). An NADPH:FAD oxidoreductase from the valinimycin producer *Streptomyces viridifaciens*. J. Biol.Chem. **272**, 23303 – 23311.
- Passantino, R., Puglia, A.M., and Chater, K.F. (1991). Additional copies of the *act*II regulatory gene induce actonorhodin production in pleiotropic *bld* mutants of *Streptomyces coelicolor* A3(2). J. Gen. Microbiol. **137**, 2059 – 2064.
- Rajgarhia, V.B., Priestley, N.D., and Strohl, W.R. (2001). The product of *dps*C confers starter unit fidelity upon the daunorubicin polyketide synthase of *Streptomyces* sp. strain C5. Metabolic Engineering **3**, 49 – 63.
- Salas, J.S., Quiros, L.M., and Hardisson, C. (1984). Pathways of glucose catabolism during germination of *Streptomyces* spores. FEMS Microbiol. Lett. **22**, 229-233.
- Savinell, J.M., and Palsson, B.O. (1992). Optimal selection of metabolic fluxes for in vivo experimental determination. I. Development of mathematical methods. J. Theor. Biol. **155**, 201 – 214.
- Stephanopoulos, G.N., Aristidou, A.A., and Nielsen, J. (1998) Metabolic Engineering: Principles and Methodologies. California: Academic Press.
- Stephanopoulos, G., and Vallino, J.J. (1991) Network rigidity and metabolic engineering in metabolite overproduction. Science **252**, 1675-1681.
- Strohl, W.R., and Connors, N.C. (1992). Significance of anthraquinone formation resulting from the cloning of actinorhodin genes in heterologous Streptomycetes. Mol. Microbiol. **6**, 147-152.

- Strohl, W.R., Bartel, P.L., Connors, N.C., Zhu, C-B., Dosch, D.C., Beale, J.M., Floss, H.G., Stutzmann-Engwall, K., Otten, S.L., and Hutchinson, C.R. (1989). Biosynthesis of natural and hybrid polyketides by anthracyclin-producing Streptomycetes. *In* “Genetics and molecular biology of industrial microorganisms” (Hershberger, C.L., Queener, S.W. and Hegeman, G., Eds.), pp 68 – 84, American Society for Microbiology, Washington.
- Surowitz, K.G., and Pfister, R.M. (1985). Glucose metabolism and pyruvate excretion by *Streptomyces alboniger*. Can. J. Microbiol. **31**, 702-706.
- Takano, E., Gramajo, H.C., Strauch, E., Andres, N., White, J., and Bibb, M.J. (1992). Transcriptional regulation of the *red*D transcriptional activator gene accounts for growth-phase-dependent production of the antibiotic undecylprodigiosin in *Streptomyces coelicolor* A3(2). Mol. Microbiol. **6**, 2797 – 2804.
- Titgemeyer, F., Walkenhorst, J., Reizer, J., Stuiver, M.H., Cui, X., and Saier, M.H., Jr. (1995). Identification and characterization of phosphoenolpyruvate:fructose phosphotransferase systems in three *Streptomyces* species. Microbiology **141**, 51 – 58.
- Tsao, S.W., Rudd, B.A.M., He, X., Chang, C., and Floss, H.G. (1985). Identification of a red pigment from *Streptomyces coelicolor* A3(2) as a mixture of prodigiosin derivatives. J. Antibiotics **38**, 128-131.
- Vallino, J.J., and Stephanopoulos, G. (1990). Flux determinations in cellular bioreaction networks: application to lysine fermentations. *In*

"Frontiers of Bioprocessing" (Sikdar, S.K., Bier, M., and Todd, P., Eds.), pp. 205 – 219, CRC Press, Boca Raton, FL.

- Vallino, J.J., and Stephanopoulos, G. (1994). Carbon flux distribution at the glucose 6-phosphate branch point in *Corynebacterium glutamicum* during lysine overproduction. Biotech. Prog. **41**, 633-646.
- van Gulik, W.M., and Heijnen, J.J. (1995). A metabolic network stoichiometry analysis of microbial growth and product formation. Biotech. Bioeng. **48**, 681-698.
- Ward, J.M., Janssen, G.R., Kieser, T., Bibb, M.J., Buttner, M.J., and Bibb, M.J. (1986). Construction and characterisation of a series of multi-copy promoter-probe plasmid vectors for *Streptomyces* using the aminoglycoside phosphotransferase gene from Tn5 as indicator. Mol. Gen. Genetics **203**, 468 – 478.
- Wasserman, H.H., Shaw, C.K., and Sykes, R.J. (1974). The biosynthesis of metacycloprodigiosin and undecyl prodigiosin. Tetrahedron Lett. **33**, 2787-2790.
- Zhu, Y., Rinzema, A., Tramper, J., and Bol, J. (1996). Medium design based on stoichiometric analysis of microbial transglutaminase production by *Streptoverticillium mobaraense*. Biotechnol. Bioeng. **50**, 291-298.
- Zhu, Y., Rinzema, A., Bonarius, H.P.J, Tramper, J., and Bol, J. (1998). Microbial transglutaminase production by *Streptoverticillium mobaraense*: Analysis of amino acid metabolism using mass balances. Enz. Microbial Technol. **23**, 216-226.

Appendix.

A list of all the reactions considered in the model is presented below. Only physiologically relevant reactions were included (*e.g.*, reactions reversible *in vitro* but not *in vivo*, or reactions occurring only under anaerobic conditions were omitted). All reactions were expressed in C-mole. Reactions 1a to 1c were employed when gluconate was the carbon source, whereas reaction 1 involves glucose as the carbon source. Reaction 36a (ACT production) was used in 102 cultures, whereas reaction 36b (RED production) was employed in 103 cultures. Arrows (→) indicate physiologically irreversible reactions, while double arrows (↔) indicate reversible reactions. The bioreaction network system obtained was solved by BioNet, a PC-based program kindly supplied by Prof. G. Stephanopoulos.

For a theoretical discussion of Metabolic Flux Analysis, see: Vallino and Stephanopoulos (1990), Savinell and Palsson (1992), van Gullik and Heijnen (1995), and Stephanopoulos *et al*. (1998).

1) GLUCOSE + 1/6ATP → GLUCOSE-6-P + 1/6ADP

1a) GLUCONATE + 1/6ATP → 6-P-GLUCONATE + 1/6ADP

1b) 6-P-GLUCONATE + 1/6NAD^+ → 5/6RIBULOSE-5-P + 1/6NADH + 1/6CO2

1c) 6-P-GLUCONATE + 1/6NADPH → GLUCOSE-6-P + 1/6$NADP^+$

2) GLUCOSE-6-P ↔ FRUCTOSE-6-P

3) FRUCTOSE-6-P + 1/6ATP → GLYCERALDEHYDE –3-P + 1/6ADP

4) GLYCERALDEHYDE -3-P + 1/3ADP + 1/3NAD^+ → 3-P-GLYCERATE + 1/3ATP + 1/3NADH

5) 3-P-GLYCERATE $\leftrightarrow$ PHOSPHOENOLPYRUVATE

6) PHOSPHOENOLPYRUVATE + 1/3ADP $\rightarrow$ PYRUVATE + 1/3ATP

7) PYRUVATE + 1/3NAD^+ $\rightarrow$ 2/3ACETYLCOA + 1/3CO_2 + 1/3NADH

8) PYRUVATE + 1/3NADH $\rightarrow$ LACTATE + 1/3NAD^+

9) ACETYLCOA + 2OXALOACETATE $\leftrightarrow$ 3ISOCITRATE

10) ISOCITRATE + 1/6$NADP^+$ $\leftrightarrow$ 5/6αOXOGLUTARATE + 1/6NADPH + 1/6CO_2

11) αOXOGLUTARATE + 1/5NAD^+ + 1/5ADP $\leftrightarrow$ 4/5SUCCINATE + 1/5CO_2 + 1/5NADH + 1/5ATP

12) SUCCINATE + 1/4FAD^+ $\leftrightarrow$ MALATE + 1/4FADH

13) MALATE + 1/4NAD^+ $\leftrightarrow$ OXALOACETATE + 1/4NADH

14) αOXOGLUTARATE $\rightarrow$ αOXOGLUTARATE (ext)

15) ISOCITRATE $\rightarrow$ CITRATE(ext)

16) PYRUVATE $\rightarrow$ PYRUVATE(ext)

17) GLUCOSE-6-P + 1/3$NADP^+$ $\rightarrow$ 5/6RIBULOSE-5-P + 1/6CO_2 + 1/3NADPH

18) RIBULOSE-5-P $\leftrightarrow$ RIBOSE-5-P

19) RIBULOSE-5-P $\leftrightarrow$ XYLULOSE-5-P

20) XYLULOSE-5-P + RIBOSE-5-P $\leftrightarrow$ 7/5SEDOHEPTULOSE-7-P + 3/5GLYCERALDEHYDE-3-P

21) SEDOHEPTULOSE-7-P + 3/7GLYCERALDEHYDE-3-P $\leftrightarrow$ 6/7FRUCTOSE-6-P + 4/7ERYTHROSE-4-P

22) XYLULOSE-5-P + 4/5ERYTHROSE-4-P $\leftrightarrow$ 6/5FRUCTOSE-6-P + 3/5GLYCERALDEHYDE-3-P

23) 3-P-GLYCERATE + 5/3GLUTAMATE + 1/3NAD^+ → SERINE + 1/3NADH + 5/3αOXOGLUTARATE

24) SERINE → 2/3GLYCINE

25) PYRUVATE + 5/6GLUTAMATE + 1/3ACETYLCOA → 5/6αOXOGLUTARATE + 1/3CO_2 + LEUCINE

26) OXALOACETATE + 5/4GLUTAMINE ↔ ASPARTATE + 5/4αOXOGLUTARATE

27) ASPARTATE + 5/12ATP + 1/2NADPH + 1/4PYRUVATE + 5/12GLUTAMATE → 1/2LYSINE + 1/3THREONINE + 5/12METHIONINE + 5/12ADP + 1/2$NADP^+$ + 1/12CO_2

28) αOXOGLUTARATE + 1/5NH_4^+ + 1/5NADPH ↔ GLUTAMATE + 1/5$NADP^+$

29) GLUTAMATE + 1/5ATP + 1/5NH_4^+ → GLUTAMINE + 1/5ADP

30) GLUTAMATE + 1/5ATP + 2/5NADPH → PROLINE + 1/5ADP + 2/5$NADP^+$

31) PHOSPHOENOLPYRUVATE + 1/3CO_2 → 4/3OXALOACETATE

32) 2NADH + O_2 + 4ADP → 4ATP + 2NAD^+

33) ATP → ADP

34) 0.03GLUCOSE-6-P + 0.011FRUCTOSE-6-P + 0.113RIBOSE-5-P + 0.036ERYTHROSE-4-P + 0.01GLYCERALDEYDE-3-P + 0.113 3-P-GLYCERATE + 0.039PHOSPHOENOLPYRUVATE + 0.094PYRUVATE + 0.165ACETYLCOA + 0.075αOXOGLUTARATE + 0.11OXALOACETATE + 0.05LYSINE + 0.2NH_4^+ + 0.031GLUTAMATE + 0.031GLUTAMINE + 0.973ATP + 0.343NADPH + 0.078NAD^+ + 0.065LEUCINE + 0.019METHIONINE + 0.024THREONINE → BIOMASS + 0.973ADP + 0.343$NADP^+$ + 0.078NADH + 0.036CO_2

35) NITRATE + 8NADH → NH_4^+ + 8NAD^+

36a) ACETYLCOA + $_{14/32}$ATP + $_{28/32}$NADPH → ACTINORHODIN + $_{14/32}$ADP + $_{28/32}$$NADP^+$

36b) $_{15/25}$PYRUVATE + $_{4/25}$ATP + $_{5/25}$$NAD^+$ + $_{6/25}$SERINE + $_{10/25}$PROLINE + $_{4/25}$GLYCINE → UNDECYLPRODIGIOSIN + $_{10/25}$$CO_2$ + $_{4/25}$ADP + $_{5/25}$NADH

Figure 1. Schematic representation of the biochemical network described in the Appendix, employed for the Metabolic Flux Analysis of *Streptomyces lividans* cultures.

Figure 2. Fluxes of substrate input (○), pentose phosphate pathway (△) and ACT or RED production (□) in P-limited chemostat cultures of *Streptomyces lividans*. Graphs **A** and **C** correspond to cultures of strain 102 with glucose or gluconate, respectively, as the carbon source, whereas graphs **B** and **D** correspond to cultures of RpdS 103 with glucose or gluconate, respectively, as the carbon source. The flux towards ACT or RED production in the control strain (■) is also presented. The fluxes were calculated by solving the bioreaction network system presented in the Appendix, using the results of the experiments described in the Text.

Figure 3. Fluxes towards ACT (△) and RED (σ) production in P-limited chemostat cultures of *Streptomyces lividans* RpdS 102 and *Streptomyces lividans* RpdS 103, respectively, as a function of the flux through the pentose phosphate pathway (X_{PPP}), with glucose (**A**) or gluconate (**B**) as carbon source. The results were obtained by solving the bioreaction network system presented in the Appendix, using the results from the experiments described in the Text.

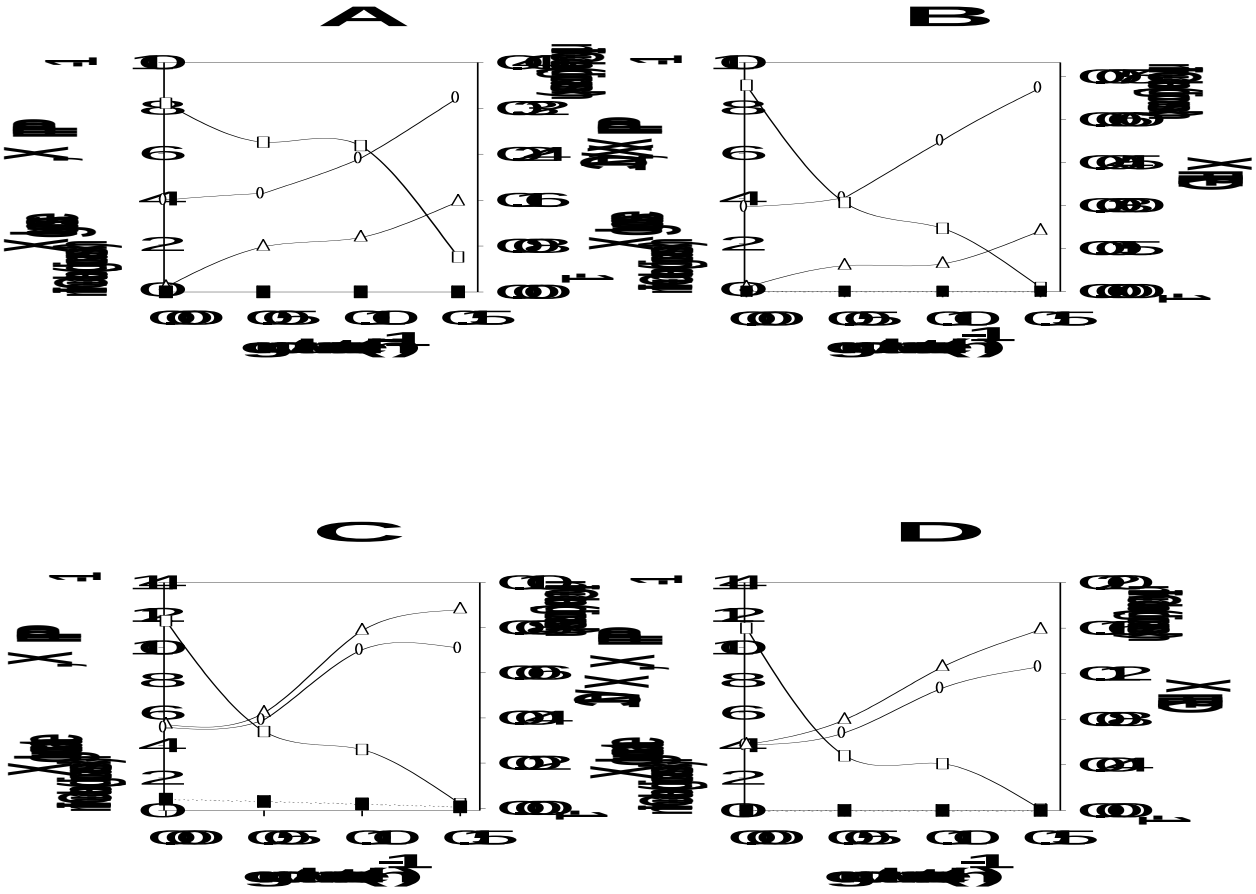
A
B
C
D

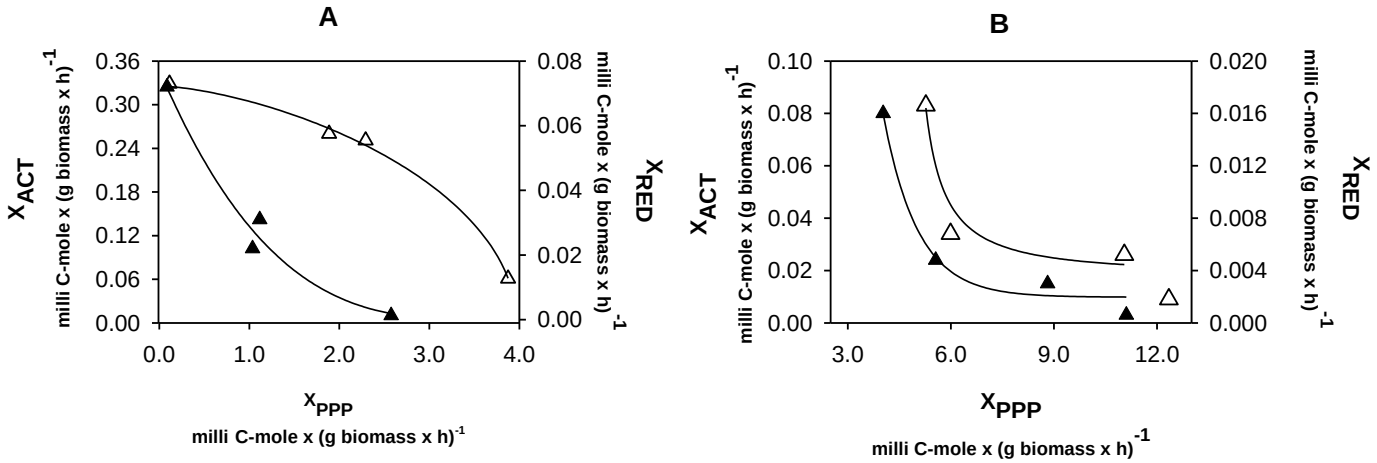
A
0.36
0.30
0.24
0.18
0.12
0.06
0.00
0.08
0.06
0.04
0.02
0.00
0.0
1.0
2.0
3.0
4.0
X_ACT
milli C-mole x (g biomass x h)^-1
X_RED
milli C-mole x (g biomass x h)^-1
X_PPP
milli C-mole x (g biomass x h)^-1
B
0.10
0.08
0.06
0.04
0.02
0.00
0.020
0.016
0.012
0.008
0.004
0.000
3.0
6.0
9.0
12.0
X_ACT
milli C-mole x (g biomass x h)^-1
X_RED
milli C-mole x (g biomass x h)^-1
X_PPP
milli C-mole x (g biomass x h)^-1

Table 1. Biomass concentration, specific rates of substrate consumption and product formation, and product yields observed in chemostat cultures of *Streptomyces lividans* RpdS 102, 103, and 105 with glucose as the C-source.

Strain	D[a]	X[b]	qCO_2[c]	qO_2[d]	q_s[e]	q_{ACT}[f]	q_{RED}[f]	$q_{\alpha KG}$[g]	q_{PYR}[g]	q_{CIT}[g]	q_{LAC}[g]	$Y_{P/S}$[h]
102	0.05	8.4	2.1	1.5	4.5	0.25	--	--	--	--	--	6.0
	0.10	6.4	2.8	2.6	6.5	0.25	--	2×10^{-4}	3×10^{-4}	--	2×10^{-4}	3.7
	0.15	4.6	3.6	2.4	8.4	0.05	--	3×10^{-4}	4×10^{-4}	--	2×10^{-4}	0.6
103	0.05	7.5	1.6	1.1	3.0	--	0.022	--	--	--	--	0.6
	0.10	5.8	2.4	1.7	6.6	--	0.040	1×10^{-4}	5×10^{-4}	--	--	0.6
	0.15	3.0	4.5	3.7	10.7	--	0.001	2×10^{-4}	7×10^{-4}	--	--	<0.01
105	0.05	6.5	1.1	0.9	3.0	--	0.001	--	--	--	--	0.03
	0.10	6.1	2.2	1.6	6.6	--	0.0005	1×10^{-4}	--	--	--	<0.01
	0.15	5.2	3.5	2.1	9.6	--	0.0005	2×10^{-4}	--	--	--	<0.01

[a]Dilution rate (h^{-1}); [b]Biomass, $g.l^{-1}$; [c]Specific CO_2 production rate, milliC-mole $\times$ $(g \times h)^{-1}$; [d]Specific O_2 consumption rate, millimole $\times$ $(g \times h)^{-1}$; [e]Specific glucose consumption rate, milliC-mole $\times$ $(g \times h)^{-1}$; [f]ACT or RED specific production rate, milliC-mole $\times$ $(g \times h)^{-1}$. [g]Specific acid(s) production rate, milliC-mole $\times$ $(g \times h)^{-1}$: αKG: α-oxoglutaric acid; PYR: pyruvic acid; CIT: citric acid; LAC: lactic acid. [h]Product (ACT or RED) yield, C-mole product $\times$ (100 C-mole consumed substrate)$^{-1}$. (--): Not detected. For all conditions a carbon recovery of 100 $\pm$ 5 % was calculated.

Table 2. Biomass concentration, specific rates of substrate consumption and product formation, and product yields observed in chemostat cultures of *Streptomyces lividans* RpdS 102, 103, and 105 with gluconate as the C-source.

Strain	D[a]	X[b]	qCO_2[c]	qO_2[d]	q_s[e]	q_{ACT}[f]	q_{RED}[f]	$q_{\alpha KG}$[g]	q_{PYR}[g]	q_{CIT}[g]	q_{LAC}[g]	$Y_{P/S}$[h]
102	0.05	6.1	2.2	1.4	5.1	0.034	--	0.26	0.28	0.15	0.03	0.7
	0.10	5.7	2.7	1.6	9.1	0.026	--	0.68	1.66	0.15	0.06	0.4
	0.15	4.3	3.6	2.1	9.7	0.002	--	0.001	0.02	0.01	0.004	0.02
103	0.05	7.7	2.0	1.2	4.8	--	0.048	0.51	0.47	0.06	0.003	1.0
	0.10	7.5	2.8	1.7	7.7	--	0.041	0.90	0.85	0.07	0.02	0.6
	0.15	3.5	3.8	2.7	8.8	--	0.001	2×10^{-4}	1×10^{-4}	--	--	0.01
105	0.05	7.4	1.6	1.1	3.7	--	0.0076	0.15	0.14	--	--	0.2
	0.10	5.4	2.5	1.2	9.5	--	0.0019	1.42	1.13	0.05	--	0.02
	0.15	4.4	2.9	1.7	12.0	--	0.0006	1.74	1.36	0.11	0.06	<0.01

[a]Dilution rate (h^{-1}); [b]Biomass, $g.l^{-1}$; [c]Specific CO_2 production rate, milliC-mole $\times$ $(g \times h)^{-1}$; [d]Specific O_2 consumption rate, millimole $O_2 \times (g \times h)^{-1}$; [e]Specific gluconate consumption rate, milliC-mole $\times$ $(g \times h)^{-1}$; [f]ACT or RED specific production rate, milliC-mole $\times$ $(g \times h^{-1})$; [g]Specific acid(s) production rate, milliC-mole $\times$ $(g \times h)^{-1}$: αKG: α-oxoglutaric acid; PYR: pyruvic acid; CIT: citric acid; LAC: lactic acid. [h]Product (ACT or RED) yield, C-mole product $\times$ (100 C-mole consumed substrate)$^{-1}$. (--): Not detected. For all conditions a carbon recovery of 100 $\pm$ 5 % was calculated.

Table 3a. Specific rates of substrate consumption and product formation, and growth rates observed in starvation experiments of *Streptomyces lividans* RpdS 102, 103, and 105 with glucose as the C-source.

Strain	growth rate	$q_{GLUCOSE}$	q_{ACT}	q_{RED}	q_{PYR}	q_{CIT}	$Y_{P/S}$
102	0.009	2.3	0.32	--	0.29	--	13.9
103	0.009	3.0	--	0.07	0.66	--	2.4
105	0.005	7.1	**--**	0.04	0.52	0.13	0.06

Growth rate in h^{-1}. $q_{GLUCOSE}$: specific glucose consumption rate; q_{ACT}: specific ACT production rate; q_{RED}: specific RED production rate; q_{PYR}: specific pyruvic acid production rate; q_{CIT}: specific citric acid production rate. Specific rates in milliC-mole $\times$ $(g\times h)^{-1}$. $Y_{P/S}$: Product (ACT or RED) yield, C-mole product $\times$ (100 C-mole consumed substrate)$^{-1}$. (--): Not detected.

Table 3b. Specific rates of substrate consumption and product formation, and growth rates observed in starvation experiments of *Streptomyces lividans* RpdS 102, 103, and 105 with gluconate as the C-source.

Strain	Growth rate	$q_{GLUCONATE}$	q_{ACT}	q_{RED}	q_{PYR}	q_{CIT}	$Y_{P/S}$
102	0.004	5.1	0.083	--	1.07	--	1.6
103	0.009	4.0	--	0.13	1.78	--	3.3
105	0.009	4.3	--	0.009	0.99	0.19	0.2

Growth rate in h^{-1}. $q_{GLUCONATE}$: specific gluconate consumption rate; q_{ACT}: specific ACT production rate; q_{RED}: specific RED production rate; q_{PYR}: specific pyruvic acid production rate; q_{CIT}: specific citric acid production rate. Specific rates in milliC-mole $\times$ $(g \times h)^{-1}$. $Y_{P/S}$: Product (ACT or RED) yield, C-mole product $\times$ (100 C-mole consumed substrate)$^{-1}$. (--): Not detected.

Table 4. Fluxes through glycolysis, and ratio of fluxes through the tricarboxylic acid cycle and glycolysis calculated by Metabolic Flux Analysis of *S. lividans* RpdS 102, 103, and 105.

Strain	growth rate	$X_{TCA}/X_{glycolysis}$		$X_{glycolysis}$	
		glucose	gluconate	glucose	gluconate
102	0	1.00	0.43	3.20	3.58
	0.05	0.57	0.46	3.14	3.43
	0.10	0.70	0.26	4.63	7.22
	0.15	0.58	0.48	6.22	6.09
103	0	1.00	0.20	3.11	2.94
	0.05	0.74	0.41	3.28	3.21
	0.10	0.73	0.35	5.65	4.91
	0.15	0.82	0.43	7.46	5.68
105	0	0.96	0.65	7.72	4.18
	0.05	0.62	0.46	2.24	3.29
	0.10	0.60	0.10	4.70	6.11
	0.15	0.58	0.04	6.94	8.03

$X_{TCA}/X_{glycolysis}$: Ratio of fluxes through TCA and Glycolysis. $X_{glycolysis}$: flux through glycolysis, expressed in milliC-mole $\times$ (g biomass $\times$ h)$^{-1}$. Growth rate in h^{-1}

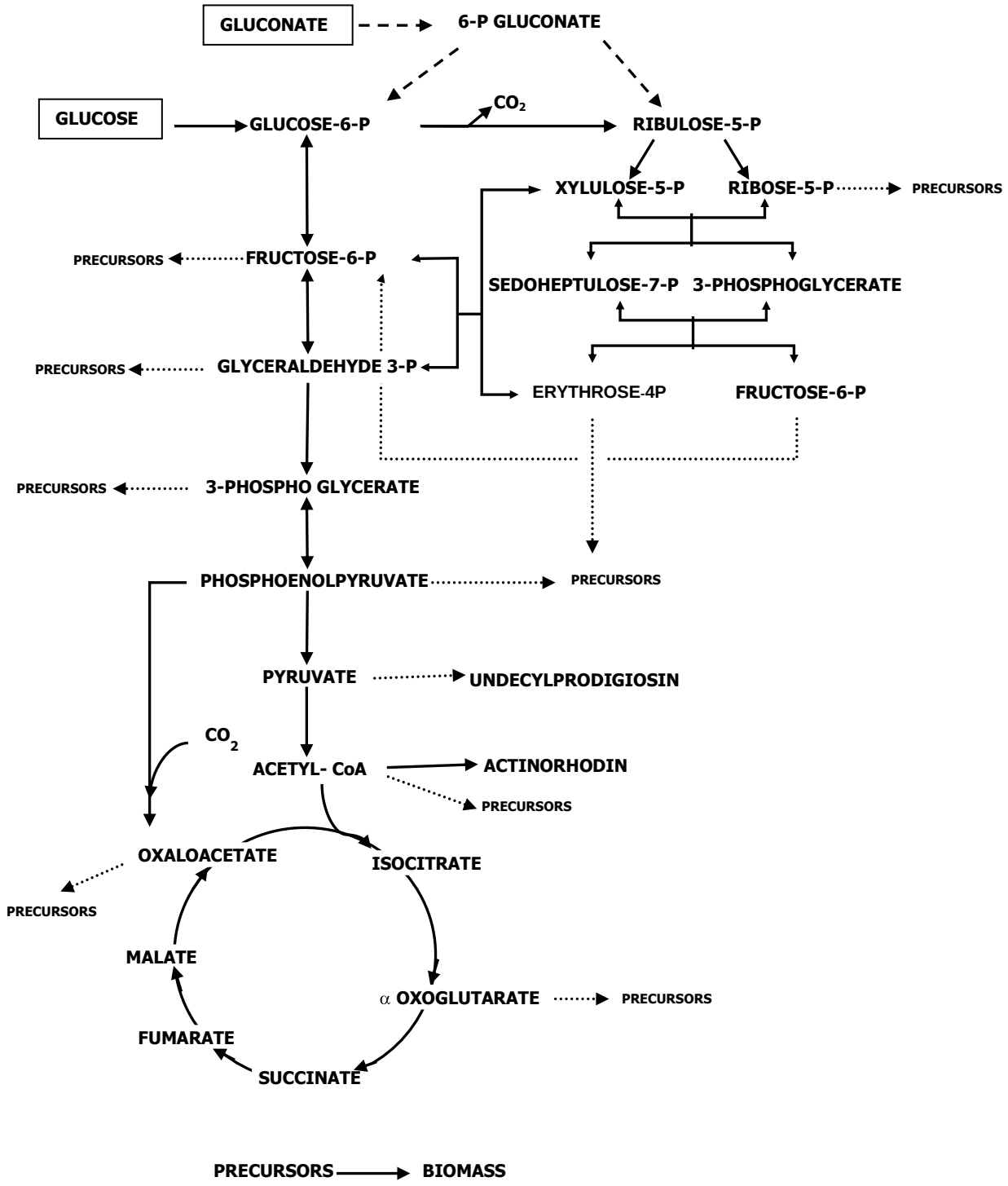
GLUCONATE
6-P GLUCONATE
GLUCOSE
GLUCOSE-6-P
CO_2
RIBULOSE-5-P
XYLULOSE-5-P
RIBOSE-5-P
PRECURSORS
PRECURSORS
FRUCTOSE-6-P
SEDOHEPTULOSE-7-P
3-PHOSPHOGLYCERATE
PRECURSORS
GLYCERALDEHYDE 3-P
ERYTHROSE-4P
FRUCTOSE-6-P
PRECURSORS
3-PHOSPHO GLYCERATE
PHOSPHOENOLPYRUVATE
PRECURSORS
PYRUVATE
UNDECYLPRODIGIOSIN
CO_2
ACETYL- CoA
ACTINORHODIN
PRECURSORS
OXALOACETATE
ISOCITRATE
PRECURSORS
MALATE
α OXOGLUTARATE
PRECURSORS
FUMARATE
SUCCINATE
PRECURSORS
BIOMASS